

## Photoionization and Ion-Radical Decay of Anthracene in a Water Swollen Nafion Network. Effect of Different Counterions on the $\text{SO}_3^-$ –Water Clusters

J. Kiwi,<sup>†</sup> M. R. Dhananjeyan,<sup>†</sup> and V. Nadtochenko<sup>\*,‡</sup>

Laboratory of Photonics and Interfaces, Department of Chemistry, Swiss Federal Institute of Technology, CH-1015 Lausanne, Switzerland, and Institute of Chemical Physics Research of Russian Academy of Sciences, Chernogolovka, Moscow district, Russian Federation 142432

Received: November 16, 2001; In Final Form: April 29, 2002

The formation of anthracene ion radicals in the  $\text{H}^+$ –,  $\text{Na}^+$ –,  $\text{Fe}^{2+}$ –, and  $\text{Fe}^{3+}$ –Nafion membrane was established by laser kinetic spectroscopy. The formation of ion radicals was observed to be due to (1) the two photon ionization of the anthracene molecule with the formation of the radical cation  $\text{An}^{+\bullet}$  radical and a fast electron scavenging by  $\text{H}^+$ ,  $\text{Na}^+$ ,  $\text{Fe}^{2+}$ , and  $\text{Fe}^{3+}$  acting as efficient electron traps in solution and (2) the quenching of the excited anthracene by  $\text{Fe}^{3+}$  that leads by a redox process to the formation of  $\text{An}^{+\bullet}$  and  $\text{Fe}^{2+}$ . It is shown that the ensuing kinetics of the ion-radical decay depends on the chemical nature of the traps. The lifetime of  $^1\text{An}$  becomes shorter after  $\text{Fe}^{2+}$  or  $\text{Fe}^{3+}$  is introduced in the Nafion. The steady-state anthracene fluorescence is quenched by  $\text{Fe}^{3+}$  or  $\text{Fe}^{2+}$  and followed the logarithmic decay law  $\ln(I_0/I)$  where the decay in solution was seen to be proportional to the  $[\text{Fe}^{3+}]$  or  $[\text{Fe}^{2+}]$ . The counterions of  $\text{SO}_3^-$ –water clusters as well as of oxygen in the reaction media strongly affect the kinetics of ion-radical reactions occurring in the Nafion membrane. The counterions and oxygen are suggested to be the traps for the generated electrons in solution. The excited state of An was shown to react with  $\text{Fe}^{3+}$  through electron transfer. Triplet excited anthracene molecules are quenched by  $\text{Fe}^{3+}$  and  $\text{Fe}^{2+}$  with rate constants  $k_q(\text{Fe}^{3+}) = (1.9 \pm 0.19) \times 10^8 \text{ M}^{-1}\text{s}^{-1}$  and  $k_q(\text{Fe}^{2+}) = (1.4 \pm 0.11) \times 10^9 \text{ M}^{-1}\text{s}^{-1}$ . Anthracene ion radicals are formed in the reaction with  $\text{Fe}^{3+}$  but not with  $\text{Fe}^{2+}$  on thermodynamic grounds.  $\text{Fe}^{2+}$  or  $\text{Fe}^{3+}$  being different chemical species quench with similar rates the An probe inside the Nafion membrane. Treatment of  $\text{Fe}^{3+}$ –Nafion with NaOH leads to precipitation of iron particles in the membrane having as consequences (1) the decrease of the observed rate for the triplet excited anthracene quenching with a concomitant decrease in the observed  $\text{An}^{+\bullet}$  yields and (2) a significant decrease of the  $\text{An}^{+\bullet}$  decay time because of the lowering of the mobility of the iron ions in solution.

### Introduction

The controlling influence of the reaction media of elementary events is currently an important subject in photochemical research.<sup>1–3</sup> The Nafion matrix as a reaction media has recently attracted much attention in photochemical research.<sup>4–12</sup> This membrane has to be an important material for the construction of pH sensors,<sup>13</sup> for copper sensing,<sup>14</sup> and also when used as probe to test the luminescence of molecules such as pyrene and  $\text{Ru}(\text{bpy})_3^{2+}$ .<sup>15–18</sup> Ion-containing polymers or Nafion are used in a variety of photochemical and electrochemical devices including fuel cells, solar energy conversion systems, and batteries.<sup>19</sup> The structure of the Nafion membrane was studied after been embedded in aqueous solutions. A network of compartments with diameters of about 40 Å containing water connected by channels with diameters of about 10 Å has been put forward to model the Nafion topology.<sup>20</sup> When it is swollen in water, the structure of Nafion resembles that of a reverse micelle. We have already examined the photo-Fenton activity of immobilized  $\text{Fe}^{3+}$  on Nafion toward the destruction of hazardous pollutants.<sup>21</sup>

The present study aims at (1) the elucidation of the photochemistry of the anthracene (An) as a probe molecule in the

Nafion matrix in the presence of various counterions surrounding the  $-\text{SO}_3^-$ –water clusters and (2) the detailed study of the photochemical reactions between anthracene and iron ions at the  $\text{SO}_3^-$ –water clusters interface. In a previous study from our laboratory, the electron-transfer reaction between methylene blue and  $\text{Fe}^{2+}$  in Nafion was investigated<sup>5</sup> where both the methylene blue and the  $\text{Fe}^{2+}$  were in the water compartment surrounding the  $\text{SO}_3^-$  groups of the Nafion. This steric arrangement is based on the hydrophilic nature of the later species. Whereas, in the present case, we reported the interaction between hydrophobic An and hydrophilic  $\text{Fe}^{2+}$  and  $\text{Fe}^{3+}$  in the Nafion membranes. It can be expected that the hydrophilic iron ions and hydrophobic An molecules are separated in the Nafion by the interface between the water compartment and the carbon-fluorinated region of the Nafion polymer chains. This approach may also provide insight into the reactivity of  $\text{Fe}^{2+}$  and the different forms of  $\text{Fe}^{3+}$  species available in the Nafion membrane. Previously, it was reported that  $\text{Fe}^{3+}$  exists in the Nafion in various forms as aqua-hydroxy iron complexes and as iron hydro/oxide precipitated particles.<sup>22–26</sup>  $\text{Fe}^{2+}$  apparently does not precipitate. Another question addressed is which is the form of the  $\text{Fe}^{3+}$  existing in the Nafion that is more reactive relative to the excited hydrophobic An, used as a probe in the hydrophobic part of the Nafion. This study addresses the question if this iron deposited on the Nafion membrane is precipitated or not as a function of the preparative technique used. The iron–iron

\* To whom correspondence should be addressed.

<sup>†</sup> Swiss Federal Institute of Technology.

<sup>‡</sup> Institute of Chemical Physics Research of Russian Academy of Sciences.

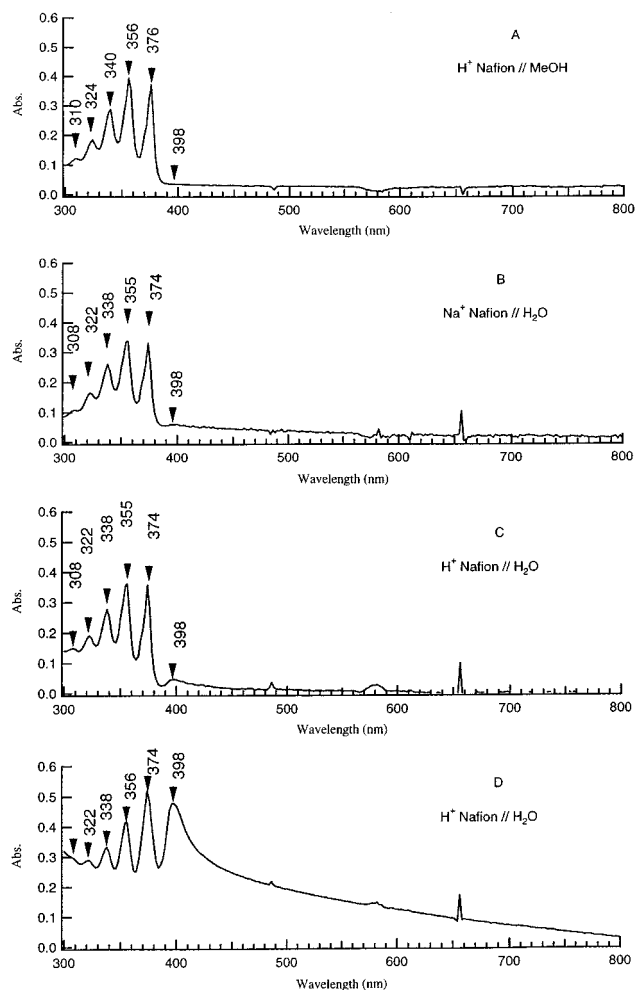


**Figure 1.** Absorption spectra of anthracene in Nafion membranes. A.  $H^+$ -Nafion swollen by methanol,  $[An] = 0.2$  mM. B.  $Na^+$ -Nafion swollen by water,  $[An] = 0.2$  mM. C.  $H^+$ -Nafion swollen by water,  $[An] = 0.2$  mM. D.  $H^+$ -Nafion swollen by water,  $[An] = 0.5$  mM.

reactivity was investigated relative to the excited anthracene and its ion radicals in solution.

### Experimental Section

**Chemicals.** The Nafion membrane 1117 was obtained from Aldrich.  $Fe(ClO_4)_3 \cdot 9H_2O$  and  $FeSO_4 \cdot 7H_2O$  were Fluka p.a. products and used without further purification as the source of  $Fe^{3+}$  and  $Fe^{2+}$  ions.

**Preparation of An Nafion Loaded Membranes.** The Nafion membranes were washed with  $H_2O_2$  (10% solutions) and subsequently with  $H_2SO_4$  (5%). Finally, repeated water was used to clean organic contaminants in the film. An was incorporated into the Nafion by dipping the film in methanolic solution with a chosen concentration of anthracene during 24 h. For experimental purposes, 5  $cm^2$  of An-Nafion loaded films were prepared from a single batch to attain the adequate reproducibility needed when comparing the different samples.

(a) *Preparation of An  $Na^+$ -Nafion Membranes.* A total of 5  $cm^2$  of An-Nafion was equilibrated with 20 mL of 1 M NaOH overnight under constant stirring. No loss of An was observed by equilibrating the film in NaOH as measured by UV-vis spectroscopy of the  $H^+$  membrane before and after NaOH addition.

(b) *Preparation of An  $Fe^{3+}$  and An  $Fe^{2+}$  -Nafion Membranes.* The 5  $cm^2$  samples of An-Nafion were dipped in various concentrations of freshly prepared  $Fe^{3+}$  and  $Fe^{2+}$  (0.05–0.12

mM solutions) of constant volume (20 mL). The solutions were deoxygenated by Ar purging, and the deoxygenated solutions were equilibrated with the Nafion loaded membranes during 24 h. No  $Fe^{3+}$  and  $Fe^{2+}$  ions were found in solution by thiocyanate and 1,10-phenanthroline, respectively, indicating that all of the  $Fe^{3+}$  and  $Fe^{2+}$  ions were incorporated into the Nafion membrane. No loss of concentration of An was also observed in both cases after  $Fe^{3+}$  and  $Fe^{2+}$  treatment. Two different types of  $Fe^{3+}$  membranes were prepared on An-Nafion substrates: (1) type I, when aqueous solutions of  $Fe^{3+}$  ion solutions were equilibrated with the  $H^+$ - or  $Na^+$ -Nafion membrane previously loaded with An and (2) type II, when membranes of type I were dipped subsequently in NaOH (1 M) solutions for 1 h. In the second case, the formation of the polymeric oxo/hydroxo iron species occurs because of the hydrolysis of  $Fe^{3+}$  complexes in the Nafion.<sup>23</sup>

**Absorption, Fluorescence, and Laser Photolysis Experiments.** The absorption spectra were recorded using a Hewlett-Packard 8452 diode-array spectrophotometer. The fluorescence was monitored with a SPEX-2 photon fluorescence spectrophotometer provided with a MX-2 baseline correction unit.

Laser photolysis was carried out with the second harmonic of a ruby laser ( $\lambda = 347$  nm, 15 mJ pulse energy, pulse width of 30 ns) operated in the Q-switched mode. An Oriel 450 W Xe lamp was used as the monitoring light source. The detection of the transient absorption changes was performed with an R 928 photomultiplier (Hamamatsu) via a grating monochromator (Bausch & Lomb). Digitization of the accumulated signals was achieved with a digital oscilloscope (Tektronix, TDS524A, Portland, Oregon). Laser experiments were carried out in 2 mm quartz cells. The excitations of the Nafion-An membranes in the appropriate solutions were carried out in the optical quartz cell perpendicular to the monitoring light.

**Estimation of the Average Number of Fe Ions in the Cluster.** The equation for  $H_{max}$  gives an estimate of the number of headgroups in a single cluster by considering the average density,  $E_w$ , Bragg  $d$  spacing, and adsorbed volume. The number of headgroups in one cluster  $H_{max}$  was calculated by

$$H_{max} = \frac{N_0 \rho}{E_w} \frac{v}{1 + V} \quad (1)$$

where  $\rho = 1.98$  g/ $cm^3$  is the Nafion density,  $E_w = 1100$  is the equivalent weight, and  $v = 4\pi R^3/3$  ( $R = d/2$ ) refers to the collision cluster volume. The Bragg  $d$  spacing used was 47  $\text{\AA}$ ,<sup>27</sup> and  $V$ , the water volume absorbed by 1  $cm^3$  of Nafion, was 0.56  $cm^3$ . Taking into account these data and  $H_{max} = 73$ , a maximum of 73/ $n$   $M^{n+}$  ions could be loaded into a single cluster. The concentration of clusters  $c$  (in units of mol/ $cm^3$ ) was calculated according to  $c = \rho/E_w H_{max}$  and was equivalent to  $2.5 \times 10^{-5}$  mol/ $cm^3$ . The average number of ions in a cluster or occupation number was defined as  $\langle \mu \rangle = c([\text{ions}]/1000)$ . Ions refers to the concentration of ions in the membrane.<sup>27</sup>

### Results and Discussions

**Absorption and Fluorescence of An in Nafion Membranes.** Figure 1 shows the absorption spectra of anthracene in the Nafion membrane in the  $H^+$  and  $Na^+$  forms swollen by methanol or water. The anthracene absorption in the water-swollen membrane is shifted by 2 nm to the blue relative to methanol-swollen one. A new red shifted band centered at around 390 nm is observed for water-swollen  $H^+$ - and  $Na^+$ -Nafion (Figure 1 parts B–D). This 390 nm band is similar to that reported in rigid media of silica, alumina, or zeolites for a stable ground-

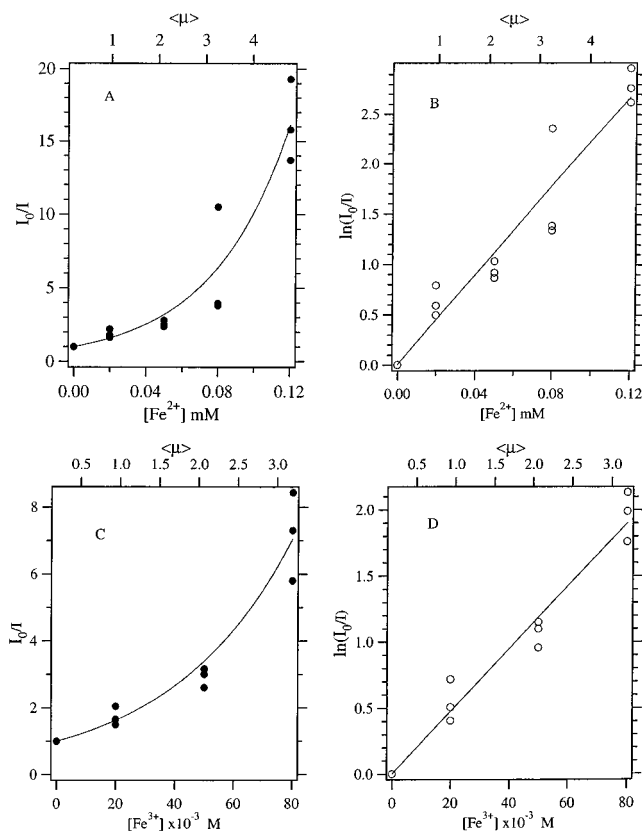


**Figure 2.** Dependence of the fluorescence intensity of anthracene in  $\text{H}^+$ -Nafion membrane as a function of the  $\text{Fe}^{2+}$  and  $\text{Fe}^{3+}$  ion concentration.  $[\text{An}] = 0.1$  mM. A. An fluorescence intensity dependence on  $[\text{Fe}^{3+}]$  in Stern–Volmer coordinates. B. An fluorescence intensity dependence on  $[\text{Fe}^{3+}]$  in logarithmic coordinates. C. An fluorescence intensity dependence on  $[\text{Fe}^{2+}]$  in Stern–Volmer coordinates. D. An fluorescence intensity dependence on  $[\text{Fe}^{2+}]$  in logarithmic coordinates.

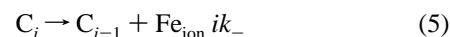
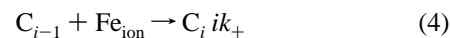
state pair between two anthracene molecules.<sup>28–35</sup> The dimer concentration increases in the order of  $\text{H}^+$ -Nafion/MeOH;  $\text{Na}^+$ -Nafion/ $\text{H}_2\text{O}$ ;  $\text{H}^+$ -Nafion/ $\text{H}_2\text{O}$  for the same amount anthracene in the Nafion (Figure 1). An increase of anthracene concentration in the membrane leads to the rise of the dimer concentration (Figure 1D). If the concentration of anthracene in the membrane is less than 0.27 mM, the formation of anthracene dimers at 390 nm is not significant. Experiments described below were performed at anthracene concentrations lower than 0.27 mM.

In the zeolites  $\text{H}^+$ -ZSM-5,  $\text{H}^+$ -mordenite, and  $\text{H}^+$ -Y, protonated anthracene formation has been recently reported.<sup>36</sup> Despite the acid nature of  $\text{H}^+$ -Nafion interior, no evidence for protonated anthracene was found in the absorption spectra or in the fluorescence spectra. Molecular anthracene absorption bands were observed to be the same in  $\text{H}^+$  and in the  $\text{Na}^+$  water-swollen Nafion membranes. This suggests that anthracene is localized outside of the water- $\text{SO}_3^-$  ionic clusters, mostly in the carbon-fluorinated part of the membrane.

Figure 2 shows the quenching of the anthracene fluorescence by hydrophilic iron ions  $\text{Fe}^{2+}$  and  $\text{Fe}^{3+}$  (type I, without NaOH treatment) in the Nafion membrane. Iron ion concentrations in Figure 2 are presented in millimolar concentrations. The average occupation number  $\langle\mu\rangle$ , defined as  $\langle\mu\rangle = (\text{Fe}^{2+} \text{ or } \text{Fe}^{3+} \text{ concentration})/(\text{concentration of the } \text{SO}_3^- \text{ -water clusters in Nafion})$  is shown in the upper  $x$  axis in Figure 2. Figure 2 shows the dependence of An fluorescence intensity on the  $\text{Fe}^{2+}$  or  $\text{Fe}^{3+}$  concentration. This dependence is significantly different from the case in homogeneous solutions following the usual Stern–

Volmer dependence for fluorescence quantum yield. This intensity dependence in Figure 2 can be approximated by the exponential  $I_0/I = \exp(-\alpha[\text{Fe}^{2+} \text{ or } \text{Fe}^{3+}])$ . For  $\text{Fe}^{2+}$ , the  $\alpha$  value is  $(22.2 \pm 1.7) 1/\text{M}$ , and for the  $\text{Fe}^{3+}$  system, this value is  $(23.7 \pm 1.4) 1/\text{M}$ . Theoretical treatments of the luminescence quenching in assemblies to calculate the equilibrium distribution of reactants (occupation statistics) have been developed.<sup>1–3</sup>

The reactions in the organized assemblies have similarities with those in Nafion such as (a) the compartmentalization of iron ions into  $\text{SO}_3^-$ -water clusters according to a similar distribution law, (b) the exchange of ions between clusters, and (c) the reaction of ions within the same cell and of molecules originally contained in different clusters through diffusion. It has also been widely reported that the structure of the Nafion membrane resembles the structure of inverted micelles.<sup>20</sup> At an average concentration of An in Nafion of 0.277 mM, the average number of An molecule per one  $\text{SO}_3^-$ -water cluster is  $1.1 \times 10^{-2}$ . Thus, the probability of one cluster being occupied by two An molecules is negligible small, and it is necessary to consider the distribution of iron ions only. This means that the An molecule in the vicinity of the particular  $\text{SO}_3^-$ -water cluster will be able to emit a photon when no iron ions are associated with that cluster. However, when one or more iron ions exist in the vicinity of the  $\text{SO}_3^-$ -water cluster, then the quantum yield of An fluorescent is infinitesimally small because they act as fluorescence quenchers. Iron-ion exchange equilibria between bulk aqueous solution and  $\text{SO}_3^-$ -Nafion cluster can be approximated as follows:



In these equations  $\text{C}_i$  is a Nafion cluster which is consisting of  $i$  of iron ions.  $k_+$  and  $k_-$  are the rate constants for iron-ions exchange between Nafion cluster and water bulk.

According to the scheme in eqs 2–5, the ion distribution between clusters can be approximated by the Poisson distribution:

$$\text{C}_i = C \langle\mu\rangle^i / i! \exp(-\langle\mu\rangle) \quad (6)$$

where  $C$  is the total concentration of  $\text{SO}_3^-$ -water clusters in the Nafion.

The concentration of empty clusters of iron ions is noted as  $\text{C}_0 = C e^{-(\mu)}$ . This is in agreement with the results presented in Figure 2 parts B and D. In this study, the simplest model has been used to show the statistical character of the quenching observed in Figure 2.

The experimental slopes of the liner plot of  $\ln(I_0/I)$  vs  $\langle\mu\rangle$  in Figure 2 parts B and D for  $\text{Fe}^{2+}$  and  $\text{Fe}^{3+}$  are close to each other, viz.,  $0.57 \pm 0.08$  for  $\text{Fe}^{2+}$  and  $0.62 \pm 0.06$  for  $\text{Fe}^{3+}$ . According to the suggested model, the slope was expected to be 1. The deviation between the experimental results and those predicted by theory is  $\sim 40\%$ . This agreement can be considered as reasonable because the  $\langle\mu\rangle$  value for iron ions in the Nafion membrane was estimated on the basis of cluster concentrations obtained from data reported for Nafion.<sup>27</sup> A similar logarithmic dependence of the fluorescence yield on the quencher concentration was observed for the quenching of methylene blue by  $\text{Fe}^{2+}$  ions<sup>5</sup> where the fluorescent methylene blue and the

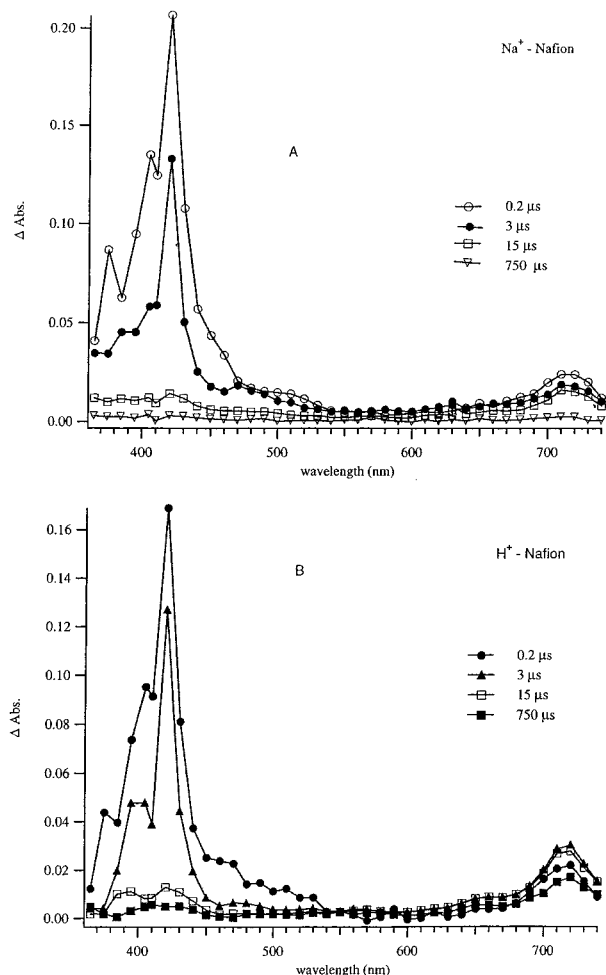


**Figure 3.** Transient absorption spectra of An in Na<sup>+</sup>- and H<sup>+</sup>-Nafion membrane water-swollen. Air oxygen was purged by Ar. A. Na<sup>+</sup>-Nafion membrane, [An] = 0.11 mM. Time delay 0.2, 3, 15, and 750 μs. B. Na<sup>+</sup>-Nafion membrane, [An] = 0.13 mM. Time delay 0.2, 3, 15, and 750 μs

quencher Fe<sup>2+</sup> were both hydrophilic species inside the SO<sub>3</sub><sup>-</sup> - water clusters. At this point, it is important to state that Fe<sup>2+</sup> or Fe<sup>3+</sup> being different chemical species produces a similar quenching of the An probe inside the Nafion.

**Intermediates Due to Laser Photolysis of An-Nafion Membranes.** Figure 3 presents the transient absorption spectra of An in the H<sup>+</sup>- and Na<sup>+</sup>-Nafion membrane. Experiments were carried out in air and in Ar atmospheres. Common features for these spectra are the strong An triplet-triplet absorption band at 420 nm and the band at 710–720 nm which is attributed to the absorption of the An ion radicals. The assignment of the absorption bands have been previously in the literature.<sup>37–41</sup> The electronic spectra of monopositive and mononegative An show similar spectral features.<sup>39,42</sup> To elucidate the nature of ion radicals, the dependence of the radical yield on the laser energy pulse and the kinetics of transient decay at the maximum of ion-radical absorption band at 710 nm will be investigated, and the results are presented in Figure 4.

Figure 4 shows the dependence of the triplet and radical yields on the energy of the laser pulse for Na<sup>+</sup>-, Fe<sup>2+</sup>-, and Fe<sup>3+</sup>-(type I)-Nafion membranes. Figure 4B shows that triplet production follows one-photon absorption. Saturation is due to (a) a large amount of absorption and (b) a significant ground state population depletion at high laser intensities. The concave curves shown in Figure 4 A for the radical yield as a function of laser energy are typical and follow a two photon

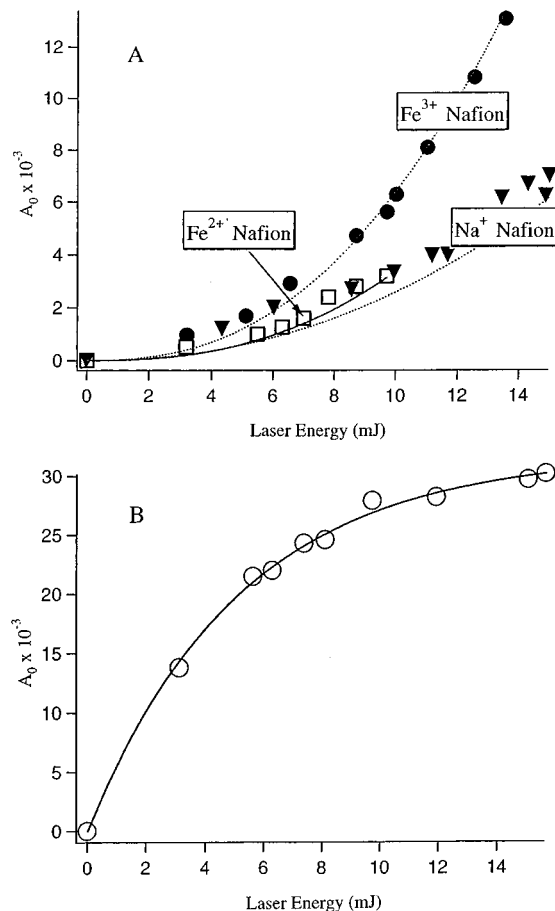


**Figure 4.** Dependence of the initial amplitude of the absorbance at 710 (A) and 420 nm (B) on the energy of the 347 nm laser pulse. Dependences of in part A were obtained for Na<sup>+</sup>-Nafion, Fe<sup>3+</sup>-Nafion (type I), and Fe<sup>2+</sup>-Nafion membranes. B shows the results for the Na<sup>+</sup>-Nafion membrane.

multiphoton process. The dependency of the radical yield immediately after laser pulse on the pulse energy by power function can be approximated by

$$A_0 \sim K(\text{energy})^{K1} \quad (7)$$

where K1 is the power coefficient for the dependency of the radical yield on the applied laser pulse energy, and then the following values were obtained: K1 = 1.8 (Na<sup>+</sup>-Nafion), K1 = 2.43 (Fe<sup>2+</sup>-Nafion), and K1 = 2.48 (Fe<sup>3+</sup>-Nafion). It follows that a two photoionization process of An predominates in the Nafion membrane leading to An<sup>•+</sup> ion-radical formation. The threshold of photoionization of tetramethylsilane (TMS) of 5.87 eV makes a two photon thermodynamically possible. In this case, the intermediate states involved are the singlet excited state of An with an energy of 3.29 eV and the triplet state of An with 1.85 eV, because the threshold in the water-swollen Nafion can be at a lower energy level than in TMS because of the polar nature of the surrounding solvent. It can also be suggested that the concentration of positive An ion radicals is higher than negative An ion radicals because of the fast capture of the photoinjected electrons can proceed on different type of traps: (a) the counteranions in SO<sub>3</sub><sup>-</sup>-water clusters e<sup>-</sup> + H<sup>+</sup> → H k<sub>sc</sub> = 4.3 × 10<sup>10</sup> M<sup>-1</sup> s<sup>-1</sup>.<sup>43,44</sup> If the H<sup>+</sup> is the counterion in the sulfonic group of the Nafion, the latter reaction proceeds with reciprocal lifetime 7.7 × 10<sup>10</sup> s<sup>-1</sup>. The concentration of the SO<sub>3</sub><sup>-</sup> group in Nafion is 1.8 M, and this concentration equals the H<sup>+</sup> concentration. (b) Taking into account that the



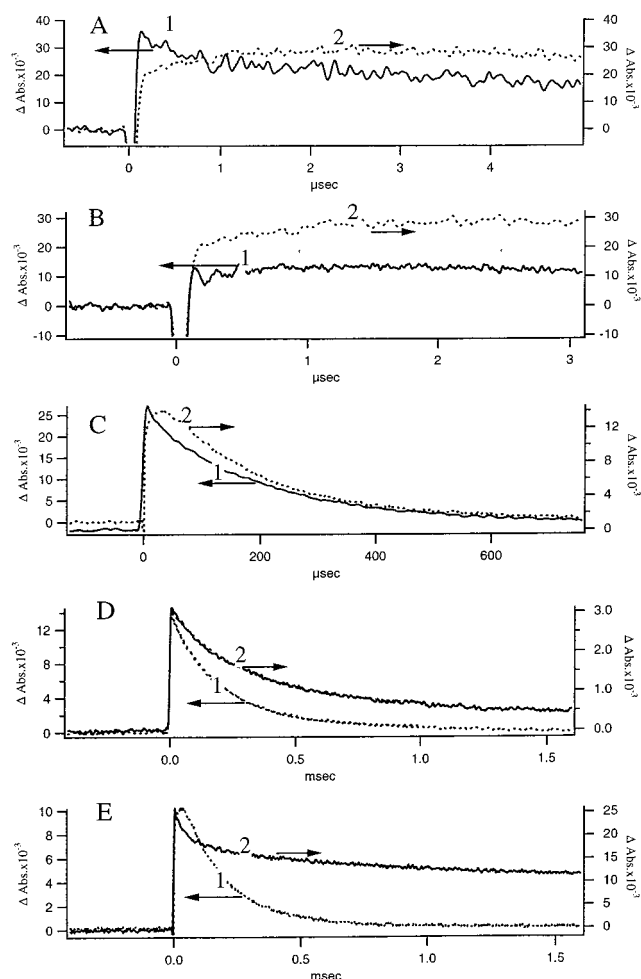
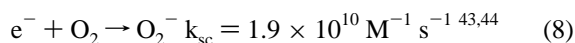


**Figure 5.** Transients at 710 nm after excitation of An by 347 nm laser pulse for  $\text{H}^+$ - and  $\text{Na}^+$ -Nafion membranes. A. Effect of  $\text{Na}^+$  or  $\text{H}^+$  counterion in  $\text{SO}_3^-$ -water clusters on the 710 nm transient at submicrosecond time scale. Air oxygen is purged by Ar. 1,  $\text{Na}^+$ -Nafion membrane; 2,  $\text{H}^+$ -Nafion membrane. B. Effect of air oxygen on the transient kinetics at 710 nm for  $\text{H}^+$ -Nafion membrane. 1, Air saturated sample; air oxygen is purged by Ar. C. Effect of  $\text{Na}^+$  or  $\text{H}^+$  counterion in  $\text{SO}_3^-$ -water clusters on the transient kinetics at 710 nm in the millisecond time scale. Air oxygen purged by Ar. 1,  $\text{Na}^+$ -Nafion membrane; 2,  $\text{H}^+$ -Nafion membrane. D. Effect of air oxygen on the transient kinetics at 710 nm for the  $\text{Na}^+$ -Nafion membrane in the millisecond time scale. 1, Air oxygen is purged by Ar.; 2, air saturated sample. E. Effect of air oxygen on the transient kinetics at 710 nm for  $\text{H}^+$ -Nafion membrane in the millisecond time scale. 1, Air oxygen is purged by Ar.; 2, air saturated sample.

$\text{O}_2$  concentration in the air is about 0.21 bar, the electron should be scavenged by  $\text{O}_2$  with a reciprocal time of  $3 \times 10^{10} \text{ s}^{-1}$  due to reaction 8:



(c)  $\text{e}^- + \text{An} \rightarrow \text{An}^- \quad k_{\text{st}} 1.2 \times 10^{12} \text{ M}^{-1} \text{ s}^{-1}$  proceeds with the rates in *n*-hexane or  $1.0 \times 10^{13} \text{ M}^{-1} \text{ s}^{-1}$  in isoctane and  $1.5 \times 10^{12} \text{ M}^{-1} \text{ s}^{-1}$  in tetramethylsilane.<sup>47,48</sup> At the concentration of  $[\text{An}] = 0.2 \text{ mM}$  in the Nafion, the reciprocal lifetime for electron scavenging by An is expected to be in the range of  $(0.24\text{--}2) \times 10^7 \text{ s}^{-1}$  taking the rate constant of  $\text{e}^-$  scavenging by An in Nafion in the same range as for hydrocarbons. The rates for the reaction of  $\text{e}^- + \text{An} \rightarrow$  in organic solvents as cited above are much higher than the diffusion rates in aqueous solutions around  $6 \times 10^9 \text{ M}^{-1} \text{ s}^{-1}$ . In good dielectric liquids, it is not possible to use  $6 \times 10^9 \text{ M}^{-1} \text{ s}^{-1}$  as the diffusion limit because

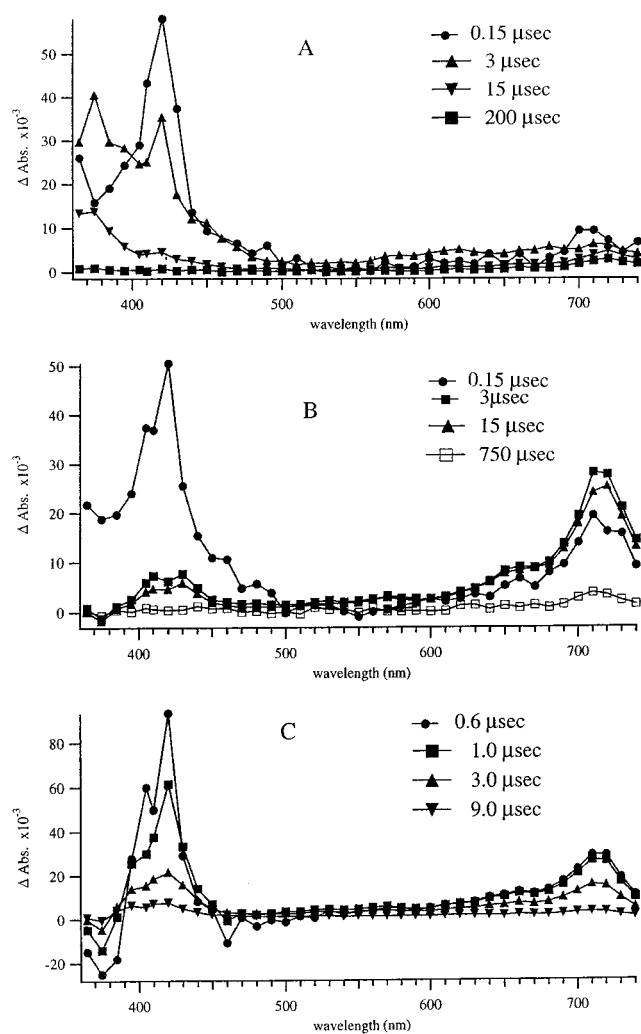


**Figure 6.** Transient absorption spectra of An in the  $\text{Fe}^{3+}$ -Nafion membranes with nonprecipitated and precipitated iron hydroxides/oxides and in the  $\text{Fe}^{2+}$ -Nafion membrane. Air saturated samples. A.  $[\text{An}] = 0.12 \text{ mM}$ .  $[\text{Fe}^{3+}] = 0.02 \text{ mM}$  type I, in the nonprecipitated form. Time delays are indicated as 0.15, 3, 15, and 750  $\mu\text{s}$ . B.  $[\text{An}] = 0.18 \text{ mM}$ .  $[\text{Fe}^{3+}] = 0.02 \text{ mM}$  type II, in the precipitated form. Time delays: 0.15, 3, 15, and 200  $\mu\text{s}$ . C.  $[\text{An}] = 0.2 \text{ mM}$ .  $[\text{Fe}^{2+}] = 0.012 \text{ mM}$ . Time delays: 0.6, 1, 3, and 9  $\mu\text{s}$ .

the electron does not behave as a conventional particle in a nonpolar media. (d) In  $\text{Na}^+$ -Nafion membranes,  $\text{e}^- + \text{Na}^+ \rightarrow \text{Na}$   $k_{\text{sc}} < 10^6 \text{ M}^{-1} \text{ s}^{-1}$ ,<sup>43,44</sup> and the reciprocal lifetime for this reaction is  $> 1.8 \times 10^6 \text{ s}^{-1}$ . (e) For the reaction  $\text{e}^- + \text{Fe}^{3+} \rightarrow \text{Fe}^{2+}$   $k_{\text{sc}} = 1.6 \times 10^{10} \text{ M}^{-1} \text{ s}^{-1}$ <sup>45</sup> at the highest  $\text{Fe}^{3+}$  concentration (30 mM), the reciprocal lifetime of electron to be scavenged by  $\text{Fe}^{3+}$  should be  $4.8 \times 10^8 \text{ s}^{-1}$ . (f) For the reaction of  $\text{Fe}^{2+}$ ,  $\text{e}^- + \text{Fe}^{2+} \rightarrow$  products,  $k_{\text{sc}} = 1.6 \times 10^8 \text{ M}^{-1} \text{ s}^{-1}$ ,<sup>46</sup> and at the highest  $\text{Fe}^{3+}$  concentration (20 mM), the reciprocal lifetime of electron to be scavenged by  $\text{Fe}^{3+}$  should be  $3.2 \times 10^6 \text{ s}^{-1}$ .

The above estimates indicate that the trapping time of the photoinjected electron is comparable or faster than time resolution of the experiment except for reaction e. No experimental evidence for trapped electrons was found in the transient spectra. This result is expected because the trapped electrons produced except in reactions (a, b, d, and e) do not present absorption in the visible range.  $\text{An}^-$  has about the same spectrum as  $\text{An}^+$ , and this was indicated above. Reaction e therefore is not able to compete with reactions (a–d). Different lifetimes should be expected for the trapped electrons in Nafion under different experimental conditions. Monopositive  $\text{An}^+$  ion radicals are formed during the duration of the laser pulse.

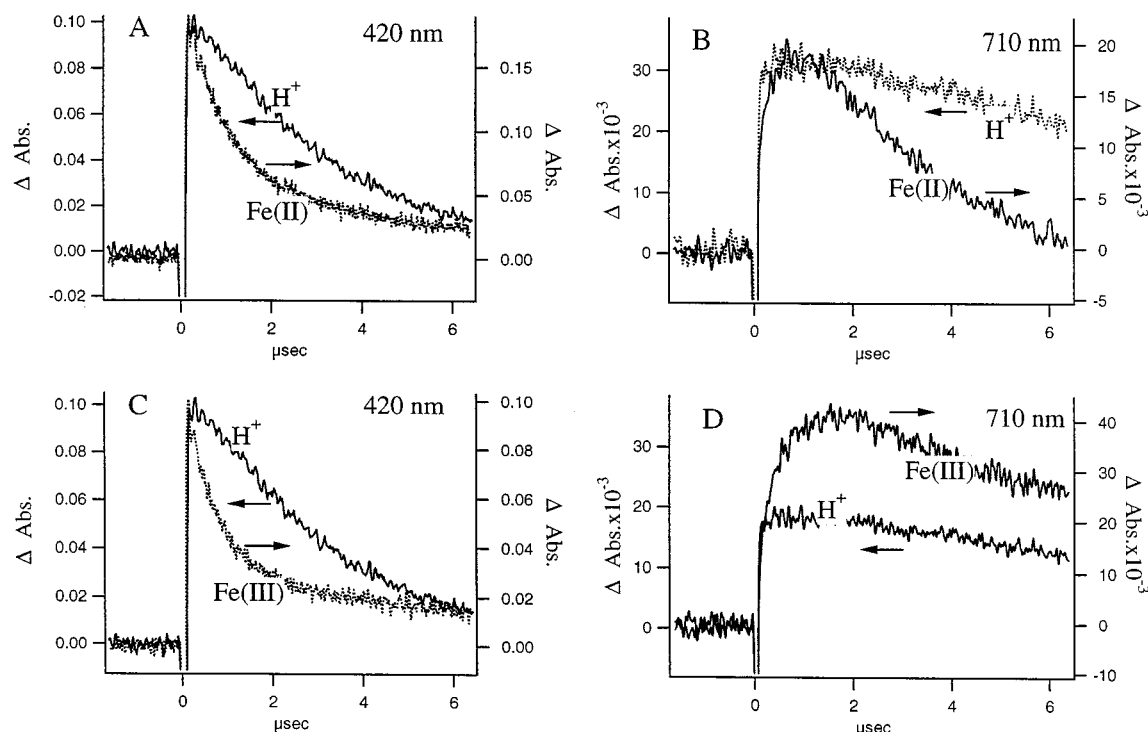


**Figure 7.** Transients for  $\text{H}^+$ -,  $\text{Fe}^{2+}$ -, and  $\text{Fe}^{3+}$ -Nafion membranes. Air saturated samples. A. At the maximum of T-T absorption band 420 nm. For  $\text{H}^+$ -Nafion  $[\text{A}] = 0.17 \text{ mM}$ ; for  $[\text{A}] = 0.15 \text{ mM}$   $[\text{Fe}^{2+}] = 0.012 \text{ mM}$ . B. At the maximum of An ion radical absorption at 710 nm. For  $\text{H}^+$ -Nafion,  $[\text{A}] = 0.17 \text{ mM}$ ; for  $[\text{A}] = 0.15 \text{ mM}$   $[\text{Fe}^{2+}] = 0.012 \text{ mM}$ . C. At the maximum of T-T absorption band 420 nm. For  $\text{H}^+$ -Nafion  $[\text{A}] = 0.17 \text{ mM}$ ; for  $[\text{A}] = 0.15 \text{ mM}$   $[\text{Fe}^{3+}] = 0.02 \text{ mM}$ . D. At the maximum of An ion radical absorption at 710 nm. For  $\text{H}^+$ -Nafion,  $[\text{A}] = 0.17 \text{ mM}$ ; for  $[\text{A}] = 0.15 \text{ mM}$   $[\text{Fe}^{3+}] = 0.02 \text{ mM}$

Figure 5 summarizes the transient curves monitored at 710 nm for samples of  $\text{H}^+$  and  $\text{Na}^+$  Nafion membranes. Figure 5A shows a qualitative difference between transient decay at 710 nm for  $\text{Na}^+$  (trace 1) and  $\text{H}^+$  (trace 2) Nafion membranes within the submicrosecond time scale. In particular, for  $\text{H}^+$  Nafion, about of 70% of total radical yield is produced during the laser pulse. A rise of absorption at 710 nm in  $\text{H}^+$  Nafion within the submicrosecond time scale shows about 30% of the total radical yield having a reciprocal rise time of  $(670 \pm 50) \text{ ns}$ . The rise of An ion radicals cannot be explained by the reaction of excited An, because it does not coincide with the lifetime of the triplet excited An. However, it can be explained by the reduction of An by different reducing agents and not necessarily only by the action due to  $\text{e}^-$ . Possible channels for the reaction are  $\text{e}^- + \text{H}^+ \rightarrow \text{H}^\bullet + \text{An} \rightarrow \text{AnH}^\bullet \rightarrow \text{An}^- + \text{H}^+$ . If the AnH has a spectrum very similar to  $\text{An}^-$ , then it is not necessary to invoke  $\text{An} \rightarrow \text{An}^- + \text{H}^+$  as a reaction channel. The estimated rate constant for  $\text{H} + \text{An} \rightarrow \text{AnH}$  should be  $k = 1/\{(670 \text{ ns})([\text{An}] = 0.2 \text{ mM})\} = 7.4 \pm 1 \times 10^9 \text{ l/M s}$ . This value is comparable to the reported rate constant for  $\text{H} + \text{An} \rightarrow \text{AnH}$  of  $3.1 \times 10^9 \text{ M}^{-1} \text{ s}^{-1}$ .<sup>49</sup> In a  $\text{Na}^+$ -Nafion membrane, no raise was observed for An ion radicals, instead a fast decay of the submicrosecond component with a lifetime of  $525 \pm 25 \text{ ns}$  was observed. This shows the different nature of the trapped  $\text{e}^-$  and the formation of H atom and a different space distribution for the ionic species due to photoionization. Air or oxygen in  $\text{H}^+$ -Nafion samples leads to the decrease of the submicrosecond rise component at 710 nm, as seen in Figure 5B.

From the above arguments, the transient decay at 710 nm can be assigned to the reaction of  $\text{An}^\bullet$  with the scavenging electron. The latter reaction involves (a) H atom and superoxide anion or  $\text{HO}_2$ , in the air saturated samples, because the  $\text{H} + \text{O}_2 \rightarrow \text{HO}_2$  is a fast reaction and  $\text{O}_2$  is a suitable scavenger for the electron or alternatively, (b) H atom only in the samples in Ar

purged solutions, and (c)  $\text{Fe}^{2+}$  in the Nafion membrane with the iron ions and with some amount of the  $\text{An}^-/\text{AnH}^\bullet$ . It was observed that in air saturated samples the lifetime of the An ion radical becomes longer than 1.5 ms, and the kinetics of radical decay did not conform to a single exponential. Superoxide anion and  $\text{HO}_2^\bullet$  radicals are suggested to be involved in secondary reactions such as dismutation processes leading to a more complex decay profile. The An ion radical decay for  $\text{H}^+$  and  $\text{Na}^+$  deoxygenated or air-saturated samples show that the decay kinetics is controlled by the chemical nature of the trapped electrons, the mobility and space distribution of the ion radicals, and various kinds of trapped electrons.

Two models have successfully described reaction kinetics in heterogeneous media: (a) the disperse kinetic model assuming a Gaussian distribution of activation energies for the kinetic decay process<sup>49</sup> and (b) the fractal dimensional model.<sup>50</sup> Model b assumes a bimolecular reaction for the radical decay on the fractal dimensional surface. The significant effect of oxygen on the radical decay kinetics suggests that the disperse kinetic model is preferred in our case when considering the radical decay, because it is difficult to explain the changes of the fractal dimension of Nafion interface when oxygen is introduced in system.

Figure 6 shows the transient absorption spectra of An Nafion samples containing  $\text{Fe}^{2+}$  or  $\text{Fe}^{3+}$  ions. A common feature for these samples is the T-T absorption band at 420 nm and the ion radical band at 710 nm. Other important observations for these systems are (1)  $\text{Fe}^{3+}$  in the nonprecipitated form in the Nafion leads to an increase of the An ion-radical yield as it is observed relative to Nafion samples with  $\text{H}^+$ ,  $\text{Na}^+$ , or  $\text{Fe}^{2+}$ , (2) a formation of hydroxo/oxo precipitated particles of  $\text{Fe}^{3+}$  in Nafion after NaOH treatment leads to a decrease of the An ion radical yield, and finally, (3)  $\text{Fe}^{2+}$  counterion in the Nafion membrane does not lead to any significant qualitative changes

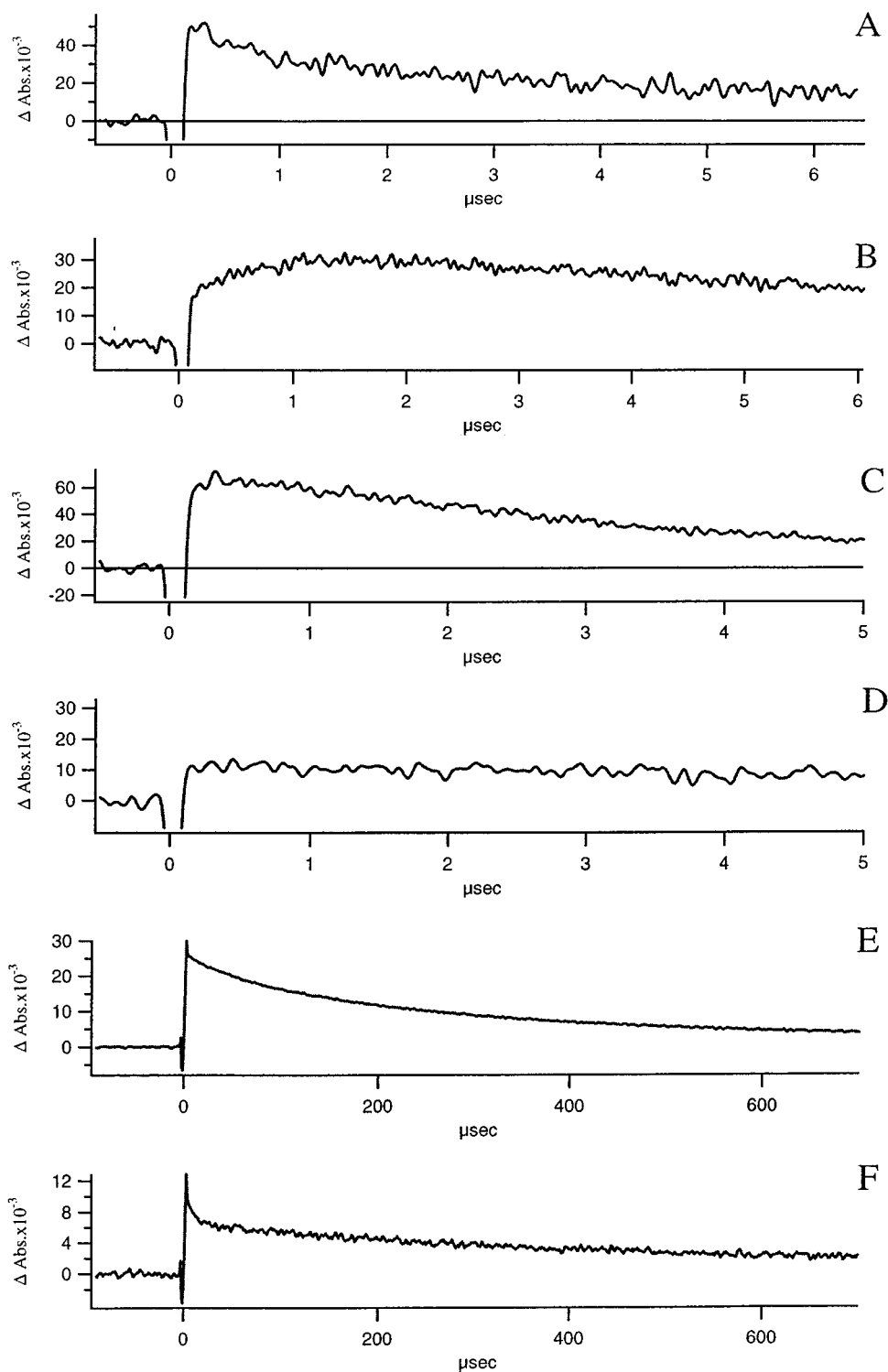


**Figure 8.** Transients for  $\text{Fe}^{3+}$  precipitated and nonprecipitated samples. Samples are purged with Ar. A. At the maximum of T-T absorption band 420 nm. B. At the maximum of An ion radical absorption at 710 nm. C. At the maximum of T-T absorption band 420 nm. D. At the maximum of An ion radical absorption at 710 nm. E. At the maximum of An ion radical absorption at 710 nm. F. At the maximum of An ion radical absorption at 710 nm

of transient spectra in the visible relative to  $\text{Na}^+$ -Nafion membrane, but it increases the rate of radical decay. The formation of An ion radicals within the laser pulse for  $\text{Fe}^{3+}$ - and  $\text{Fe}^{2+}$ -Nafion samples is due to two photon ionization and to a lesser degree to the electron transfer due the quenching of singlet excited An by iron ions.

The observations stated above indicate that triplet excited  $^3\text{An}$  can react with  $\text{Fe}^{3+}$  through electron transfer. This is confirmed by the analysis and comparison of the transient curves

for  $\text{H}^+$ -,  $\text{Fe}^{3+}$ -, and  $\text{Fe}^{2+}$ -Nafion samples shown in Figure 7 as well as for  $\text{Fe}^{3+}$  nonprecipitated (type I) and  $\text{Fe}^{3+}$  precipitated (type II) samples in Figure 8. A quenching of triplet excited An by  $\text{Fe}^{2+}$  or  $\text{Fe}^{3+}$  (type I) is demonstrated in Figure 7 parts A and C. The lifetime of  $^3\text{An}$  becomes shorter after  $\text{Fe}^{2+}$  or  $\text{Fe}^{3+}$  (type I) was introduced in the Nafion. A prominent rise of An ion radicals at 710 nm (Figure 7D) is observed when  $\text{Fe}^{3+}$  is in the Nafion. The ion-radical rise time coincides with the time decay of triplet excited  $^3\text{An}$  (Figure 7C). This is

**TABLE 1: Free Energy of Electron Transfer Reactions of Singlet or Triplet An with Iron Ions**

reactions	G (eV)
(A) An <sup>S1</sup> + Fe <sup>2+</sup> → An <sup>-</sup> + Fe <sup>3+</sup>	-0.66 eV <sup>a</sup>
(B) <sup>T</sup> An + Fe <sup>2+</sup> → An <sup>-</sup> + Fe <sup>3+</sup>	+0.66 eV <sup>a</sup>
(C) An <sup>S1</sup> + Fe <sup>3+</sup> → An <sup>+</sup> + Fe <sup>2+</sup>	-3.11 eV <sup>a</sup>
(D) <sup>T</sup> An + Fe <sup>3+</sup> → An <sup>+</sup> + Fe <sup>2+</sup>	-1.62 eV <sup>a</sup>

evidence that <sup>T</sup>An is quenched through electron transfer to Fe<sup>3+</sup> (reaction C in Table 1). Fe<sup>2+</sup> also quenches <sup>T</sup>An as seen from Figure 7A but without formation of An ion radicals (see Figure 7B). The free energy of the electron-transfer reactions of the singlet or triplet excited An with Fe<sup>2+</sup> and Fe<sup>3+</sup> are summarized in Table 1 below. This free energy was estimated by eq 9:

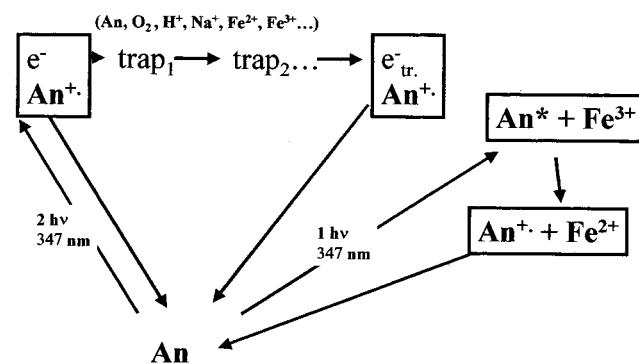
$$\Delta G = E_{1/2}(\text{ox}/\text{ox}^+) - E_{1/2}(\text{red}/\text{red}^-) - E^* \quad (9)$$

where E\* is the excitation energy of the singlet (E\*(An<sup>S1</sup>) = 3.31 eV<sup>51</sup> or triplet (E\*(<sup>T</sup>An) = 1.82 eV<sup>51</sup>) state of An. E<sub>1/2</sub>(Fe<sup>2+</sup>/Fe<sup>3+</sup>) = +0.53 eV (vs SCE).<sup>52</sup> E<sub>1/2</sub>(A<sup>-</sup>/A) = -1.92 eV (vs SCE).<sup>52</sup> E<sub>1/2</sub>(A/A<sup>+</sup>) = +0.73 eV (vs SCE)<sup>52</sup>

Table 1 shows that the electron transfer between triplet excited <sup>T</sup>An and Fe<sup>2+</sup> is thermodynamically prohibited but is allowed in the case of <sup>T</sup>An and Fe<sup>3+</sup>. These conclusions are in agreement with the experiments.

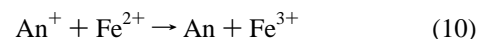
Figure 8 shows an effect of formation of the precipitated Fe<sup>3+</sup> particles in the Nafion membrane on the <sup>T</sup>An decay. A formation of the Fe<sup>3+</sup> particles leads to (1) a significant decrease of the decay rate of the triplet state <sup>T</sup>An relative to the nonprecipitated form as seen from comparison of transients in Figure 8 parts A and C. (2) At the submicrosecond time scale, the transient rise at 710 nm disappears if Fe<sup>3+</sup> precipitates (compare Figure 8 parts B and D). It indicates that <sup>T</sup>An quenching by precipitated Fe<sup>3+</sup> (type II) does not lead to a significant value of the An ions formation. Finally, (3) a precipitation of Fe<sup>3+</sup> (type II) gives a long-lived tail in the kinetics of ion-radical decay (Figure 8 parts E and F) in comparison with nonprecipitated Fe<sup>3+</sup> (type I) within the millisecond time scale. It qualitatively demonstrates how scavenging of photo-injected electrons by precipitated Fe<sup>3+</sup> particles affects the subsequent recombination of An<sup>+</sup> and the reduced forms of iron. The mechanism of growth and distribution of precipitated particles has been considered elsewhere.<sup>23;53</sup> For nonprecipitated samples, Fe<sup>3+</sup> exists mostly in the form of mono- and binuclear aqua complexes, whereas in the precipitated samples, it is found in the form of iron oxide nanoparticles. These results show that iron oxide nanoparticles are less effective quenchers of the triplet excited An and in the scavenging of electrons. Iron oxide particles have been observed to react slower with An<sup>+</sup> radicals relative to the reaction of triplet An with Fe<sup>3+</sup>-aqua complexes. This applies also to the reaction of An<sup>+</sup> with Fe<sup>2+</sup> in solution after the electron has been scavenged by Fe<sup>3+</sup>. The present results with precipitated Fe<sup>3+</sup> exhibit the effect of iron ions mobility on both the quenching rate of <sup>T</sup>An states and the rate of decay rate of An<sup>+</sup> radicals.

The dependence of the An<sup>T1</sup> lifetime and the rise time of An<sup>+</sup> formation on the Fe<sup>3+</sup> concentration are described by the Stern-Volmer relation. The rate constants found are k<sub>q</sub>(Fe<sup>3+</sup>) = (1.9 ± 0.19) × 10<sup>8</sup> for triplet decay at 420 nm and (2.0 ± 0.015) × 10<sup>8</sup> for the radical rise at 710 nm in (M s)<sup>-1</sup>. The almost coincidence of these two values can be considered as a quenching due to the reaction C in Table 1. For reaction B in Table 1, k<sub>q</sub>(Fe<sup>2+</sup>) = (1.4 ± 0.11) 10<sup>9</sup> (M s)<sup>-1</sup>. A high value of k<sub>q</sub>(Fe<sup>2+</sup>) indicates that Fe<sup>2+</sup> ions have high mobility in the SO<sub>3</sub><sup>-</sup>-water clusters. The rate constant k<sub>q</sub>(Fe<sup>2+</sup>) is about four times less than diffusion control rate constant in water estimated

**SCHEME 1**

as 6 × 10<sup>9</sup> (M s)<sup>-1</sup>. This is consistent with Mössbauer spectroscopy experiments showing that the polymer matrix had essentially no influence on the cations present in aqueous

The transient absorption decay at 710 nm is accelerated when Fe<sup>2+</sup> is introduced in the membrane (Figure 7B). The time of the radical decay correlates with the concentration of Fe<sup>2+</sup>, because the higher concentration of Fe<sup>2+</sup> used the shorter the radical lifetime was. It is the reduction of the positive ion-radical An<sup>+</sup> by Fe<sup>2+</sup>:



The estimated rate constant of this reaction is 1.5 × 10<sup>9</sup> (M s)<sup>-1</sup> that is very close to the value stated above for k<sub>q</sub>(Fe<sup>2+</sup>). This rate constant is comparable to the limit of diffusion control constant in aqueous solution.

## Conclusions

Anthracene immersed in fluorocarbon region of the Nafion membrane with different counterions of SO<sub>3</sub><sup>-</sup>-water clusters has been photoionized through two photon mechanism by 347 nm laser quanta. Singlet and triplet excited An molecules are quenched by Fe<sup>3+</sup> or Fe<sup>2+</sup> ions from the SO<sub>3</sub><sup>-</sup>-water clusters interior. In the case of nonprecipitated Fe<sup>3+</sup> in the Nafion, interfacial electron transfer occurs. The Fe<sup>2+</sup> ion reduces the An cation radicals accelerating its decay. These processes are summarized in Scheme 1.

**Acknowledgment.** This work was financially supported by Grant 00-03-32254 of the Russian Foundation of Basic Research and by the KTI/CTI TOP NANO 21 Project 5320.1 TNS, Bern, Switzerland.

## References and Notes

- Barzykin, A. V.; Tahiya, M. *Heterogen. Chem. Rev.* **1996**, *3*, 105.
- Kalyanasundaram, K. *Photochemistry in Microheterogeneous systems*; Academic Press: New York, 1987.
- Thomas, J. K. *The Chemistry of Excitation at Interfaces*; American Chemical Society: Washington, DC, 1984.
- Niu, E.-P.; Mau, A. W. H.; Chigginio, K. P. *Aust. J. Chem.* **1991**, *44*, 695-704.
- Kiwi, J.; Denisov, N. N.; Nadtochenko, V. A. *J. Phys. Chem. B* **2001**, *103*, 9141.
- Tung, C. H.; Wu, L. Z.; Zhang, L. P.; Li, H. R.; Yi, X. Y.; Ming, K. S.; Yuan, Z. Y.; Guan, J. Q.; Wang, H. W.; Ying, Y. M.; Xu, X. H. *Pure Appl. Chem.* **2000**, *72*, 2289-2298.
- Garcia-Fresnadillo, D.; Marazuela, M. D.; Moreno-Bondi, M. C.; Orellana, G. *Langmuir* **1999**, *15*, 6451-6459.
- Mazzetto, S. E.; de Carvalho, I. M. M.; Gehlen, M. H. *J. Lumin.* **1998**, *79*, 47-53.
- Inoue, H.; Urquhart, R. S.; Nagamura, T.; Grieser, F.; Sakaguchi, H.; Furlong, D. N. *Colloids Surf. A-Physicochem. Eng. Aspects* **1997**, *126*, 197-208.
- John, S. A.; Ramaraj, R. *J. Appl. Polym. Sci.* **1997**, *65*, 777-787.



- (11) Rabani, J.; Behar, D. *J. Phys. Chem.* **1995**, *99*, 11531–11536.
- (12) Niu, E.; Ghiggino, K. P.; Mau, A. W. H.; Sasse, W. H. F. *J. Lumin.* **1988**, *40-1*, 563–564.
- (13) Chan, C. M.; Fung, C. S.; Wong, K. Y.; Lo, W. *Analyst* **1998**, *123*, 1843.
- (14) Rolinski, O. M.; Hartrick, D. A.; Volkmer, A.; Birch, D. J. S. *J. Fluoresc.* **1997**, *7*, 207.
- (15) Sabatani, E.; Nikol, H. D.; Gray, H. B.; Anson, F. C. *J. Am. Chem. Soc.* **1996**, *118*, 1158–11.
- (16) Colon, J. L.; Martin, C. R. *Langmuir* **1993**, *9*, 1066–1070.
- (17) Blatt, E.; Launikonis, A.; Mau, A. W. H.; Sasse, W. H. F. *Aust. J. Chem.* **1987**, *40*, 1–12.
- (18) Szentrimay, M. N.; Prieto, N. E.; Martin, C. R. *J. Phys. Chem.* **1985**, *89*, 3017–3023.
- (19) Heitner-Wirguin, C. *J. Membrane Sci.* **1996**, *120*, 1.
- (20) Gierke, T. D.; Munn, E.; Wilson, F. C. *J. Polym. Sci., Polym. Phys. Ed.* **1981**, *19*, 1687.
- (21) Fernandez, J.; Bandara, J.; Lopez, A.; Buffat, Ph.; Kiwi, J. *Langmuir* **1999**, *15*, 185.
- (22) Haruki, R.; Seto, M.; Kitao, S.; Yoda, Y.; Maeda, Y. *J. Phys. Soc. Jpn.* **2000**, *69*, 4049–4054.
- (23) Chibirova, F. K.; Zakharin, D. S.; Sedov, V. E.; Timashev, S. F.; Popkov, Y. M.; Reiman, S. I. *Khim. Fizika* **1987**, *6*, 1137–1145.
- (24) Meagher, A.; Rodmacq, B. *New J. Chem.* **1988**, *12*, 961–964.
- (25) Meagher, A. *Inorg. Chim. Acta* **1988**, *146*, 19–23.
- (26) Meagher, A.; Rodmacq, B.; Coey, J. M. D.; Pineri, M. *React. Polym.* **1984**, *2*, 51–59.
- (27) Lee, P. S.; Meisel, J. *J. Am. Chem. Soc.* **1980**, *102*, 5477.
- (28) Dabestani, R.; Ellis, K. J.; Sigman, M. E. *J. Photochem. Photobiol. A: Chem.* **1995**, *86*, 231–239.
- (29) Dabestani, R.; Higgin, J.; Stephenson, D.; Ivanov, I. N.; Sigman, M. E. *J. Phys. Chem. B* **2000**, *104*, 10235–10241.
- (30) Ferguson, J.; Mau, A. W. H.; Morris, J. M. *Aust. J. Chem.* **1973**, *26*, 91–102.
- (31) Ferguson, J.; Mau, A. W. H.; Morris, J. M. *Aust. J. Chem.* **1973**, *26*, 13–110.
- (32) Ferguson, J. *Chem. Rev.* **1986**, *86*, 957–981.
- (33) Ford, W. E.; Kamat, P. V. *J. Phys. Chem.* **1989**, *93*, 6423.
- (34) Hashimoto, S.; Ikuta, S.; Tsuyoshi, A.; Hiroshi, M. *Langmuir* **1998**, *14*, 4284–4291.
- (35) Hashimoto, S.; Miyashita, T.; Hagiri, M. *J. Phys. Chem. B* **2001**, *103*, 9149–9155.
- (36) Liu, X.; Iu, K.-K.; Thomas, J. K.; He, H.; Klinowski, J. *J. Am. Chem. Soc.* **1994**, *116*, 11811–11818.
- (37) Iu, K. K.; Liu, X. S.; Thomas, J. K. *Chem. Phys. Lett.* **1991**, *186*, 198–203.
- (38) Iu, K. K.; Thomas, J. K. *J. Phys. Chem.* **1991**, *95*, 506–509.
- (39) Shida, T. *Physical Sciences Data 34, Electronic Absorption Spectra of Radical Ions*; Elsevier: New York, 1988; p 69.
- (40) Worrall, D. R.; Williams, S. L.; Wilkinson, F. *J. Phys. Chem. B* **1997**, *101*, 4709–4716.
- (41) Oelkrug, D.; Reich, S.; Wilkinson, F.; Leicester, P. A. *J. Phys. Chem.* **1991**, *95*, 269–274.
- (42) Aalbersberg, W.; Hoijsink, G. J.; Mackor, E. L.; Weijland, W. P. *J. Chem. Phys.* **1959**, *30*, 3049.
- (43) Pikaev, A. K. *Pulse radiolysis of water and aqueous solutions*; English ed.; Indiana University Press: Bloomington, IN, 1967.
- (44) Woods, R. J.; Pikaev, A. K. *Applied radiation chemistry: radiation processing*, Wiley: New York, 1994.
- (45) Jonah, C. D.; Miller, J. R.; Matheson, M. S. *J. Phys. Chem.* **1977**, *81*, 1618–1622.
- (46) Baxendale, J. H.; Fielden, E. M.; Keene, J. P. *Proc. R. Soc. (London) Ser. A* **1965**, *286*, 320–336.
- (47) Balakin, A. A.; Lukin, L. V.; Tolmachev, A. V.; Yakovlev, B. S. *Opt. Spectrosc. (USSR)* **1981**, *50*, 161–164.
- (48) Yakovlev, B. S.; Boriev, I. A.; Balakin, A. A. *J. Radiat. Phys. Chem.* **1974**, *6*, 23.
- (49) Albery, W. J.; Bartlett, P. N.; Wilde, C. P.; Darwent, J. R. *J. Am. Chem. Soc.* **1985**, *107*, 1854.
- (50) Oelkrug, D.; Uhl, S.; Wilkinson, F.; Willsher, C. J. *J. Phys. Chem.* **1989**, *93*, 4551.
- (51) Vauthey, V.; Haselba, E.; Suppan, P. *J. Phys. Chem.* **1987**, *70*, 0, 4709.
- (52) *CRC Handbook of Chemistry and Physics*, 58 ed.; CRC Press: Boca Raton, FL, 1977.
- (53) Chibirova, F. K.; Zakharin, D. S.; Timashev, S. F.; Popkov, Y. M.; Sedov, V. E.; Kornilova, A. A.; Reiman, S. I. *Z. Fiz. Khim.* **2001**, *62*, 645–651.